

# Structure and State of H<sub>2</sub>O in Reversed Micelles. 3.

M. Wong,\* J. K. Thomas, and T. Nowak

*Contribution from the Department of Chemistry and Radiation Laboratory,  
University of Notre Dame, Notre Dame, Indiana 46556. Received January 24, 1977*

**Abstract:** The structure and state of water in the reversed micellar system, sodium diisooctyl sulfosuccinate/H<sub>2</sub>O/heptane was investigated by both <sup>1</sup>H and <sup>23</sup>Na NMR spectroscopy. The <sup>1</sup>H NMR spectrum of H<sub>2</sub>O exhibits a downfield chemical shift with increasing water content of the system, gradually approaching that of ordinary water. This suggests a minimal amount of hydrogen bonding present in the micellar water phase at low water content. With increasing water content of this system, both the spin-lattice relaxation rates ( $1/T_1$ ) and spin-spin relaxation rates ( $1/T_2$ ) of <sup>1</sup>H of water decrease significantly up to 1% H<sub>2</sub>O, and then decrease much slower with further addition of water. A simple calculation of the rotational correlation time  $\tau_c$  from  $T_1$  demonstrates that the water molecules are highly immobilized in small water pools due to strong ion-dipole interaction with counter ions. On completion of the solvation shell of the counter ion (i.e., 1% H<sub>2</sub>O or H<sub>2</sub>O/Na<sup>+</sup>  $\approx$  6), the rigidity of the micellar core is greatly reduced. <sup>23</sup>Na NMR measurements show an analogous decrease in the  $1/T_2$  with increasing H<sub>2</sub>O content. In the largest water pool, viz. 6% H<sub>2</sub>O, it is estimated that an upper limit of 28% of the Na<sup>+</sup> is dissociated from the sulfosuccinate head group. The electronic absorption spectrum of iodide ion in the above systems is quite different from that in bulk water. The intensity of the spectrum increases with increasing water content. These data are also interpreted in terms of a decreased rigidity and increased hydrogen bonding of the micellar water pool with increasing water content.

## I. Introduction

The investigation of reversed micellar systems has received considerable attention over the past few years.<sup>1-4</sup> Reversed micelles are present in solutions of various amphiphiles in nonpolar organic solvents. Some reversed micelles can solubilize relatively large amounts of water in the micelle center. This provides a unique opportunity to study different aggregations of water molecules and the interaction of molecules with the surrounding macromolecules. These systems are thought to resemble pockets of water in bioaggregates (biomembranes, mitochondria,<sup>5</sup> etc.).

Earlier studies<sup>6</sup> have investigated the effects of the water phase in reversed micelles of sodium diisooctyl sulfosuccinate (AOT)/H<sub>2</sub>O/heptane on fluorescent properties of the environmentally sensitive probe, 1,8-anilinonaphthalenesulfonate (ANS). The nature of water bubbles in reversed micelles was found to be quite different from that of ordinary bulk water. Such differences have also been recently detected by calorimetric measurements of reversed micelle systems of AOT.<sup>7</sup> Reactions were also studied by pulse radiolysis and laser photolysis. The water phase was found to dramatically catalyze or inhibit reactions depending on the accessibility of both reactants in the presence of the micelle.

Since these systems show several unique features, it is of interest to investigate the state and nature of water in reversed micelles in more detail. <sup>1</sup>H NMR spectroscopy was used since the chemical shift and relaxation mechanisms of proton nuclei are very sensitive to their surrounding environment. <sup>23</sup>Na NMR spectroscopy was also used to investigate the relaxation mechanism of the counter ions, Na<sup>+</sup>, which are in contact with the center aqueous core and the micellar surface. Information on the specific interaction between the counter ion and the solubilized water molecules as well as counter ion binding to the micellar surface are also obtained. The UV absorption spectrum of iodide ion, which is sensitive to the solution sphere, is also investigated in several sizes of water pools in reversed micelles. The data reflect the nature of the water pools in the reversed micelles.

## II. Experimental Section

Sodium diisooctyl sulfosuccinate was obtained from American Cyanamid Co. The material was purified as previously described.<sup>6</sup> High resolution <sup>1</sup>H and <sup>23</sup>Na NMR spectra and  $T_1$  measurements were carried out with a Varian XL-100-15 NMR spectrometer equipped with Nicolet TT-100 Fourier transform accessories. The <sup>1</sup>H

and <sup>23</sup>Na spectra were recorded using C<sub>7</sub>D<sub>16</sub> and C<sub>7</sub>H<sub>16</sub> as solvents, respectively. The instrument was operated at a frequency of 100.1 and 26.65 MHz for <sup>1</sup>H and <sup>23</sup>Na, respectively, and the spectrometer was field locked on the solvent deuterium resonance for <sup>1</sup>H spectra and was unlocked for <sup>23</sup>Na spectra. Calibration of <sup>1</sup>H chemical shift was achieved by using 1% Me<sub>4</sub>Si in CDCl<sub>3</sub> as an external standard. The <sup>1</sup>H and <sup>23</sup>Na NMR spectra were obtained in the Fourier transform (FT) mode using pulsed methods. The pulse widths used were 20 and 80  $\mu$ s for <sup>1</sup>H and <sup>23</sup>Na NMR spectra, respectively.

For the <sup>1</sup>H NMR  $T_1$  (spin-lattice relaxation time) measurements, the inversion recovery method involving a 180°,  $\tau$ , 90° sequence was used.<sup>8</sup> The 90° pulse width had a 22- $\mu$ s duration. Ten scans were accumulated before Fourier transformation. Higher numbers of scans were used on low water content samples in order to achieve a better signal to noise ratio.

## III. Results and Discussion

AOT molecules in a 3% AOT solution in heptane or dodecane are completely associated into uniformly sized micellar assemblies, each containing 23 AOT molecules. The structure of such an aggregate is slightly asymmetric and may be represented by a rounded cylinder with a rod length of 33.4 Å and a cylindrical diameter of 23.9 Å. The degree of asymmetry is greatly reduced in the presence of water where a spherical pool forms in the micellar center. The aqueous core is surrounded by a layer of AOT molecules resulting in the configuration of Figure 1. The total micellar radius  $R$  is composed of the length of an AOT molecule (11 Å) and the radius of the water pool which can be calculated from  $r$  (Å) =  $36.65v/g$ , where  $v$  and  $g$  are the volume and weight percentage of water and AOT, respectively. The validity of the above equation has been verified by ultracentrifugal and light scattering measurements.<sup>9</sup> Table I lists  $R$  values and micellar compositions for relevant AOT solutions used in the present experiments.

**The Structure and State of H<sub>2</sub>O in Reversed Micelles. <sup>1</sup>H NMR Studies.** The <sup>1</sup>H NMR spectrum of 3% AOT/0.8% H<sub>2</sub>O/C<sub>7</sub>D<sub>16</sub> is shown in Figure 2. The spectrum consists of six resonance peaks attributed to CH<sub>3</sub> ( $\delta$  1.04), CH<sub>2</sub> ( $\delta$  1.45), CH<sub>2</sub>COO ( $\delta$  2.02), SO<sub>3</sub>CH ( $\delta$  4.18), COOCH<sub>2</sub> ( $\delta$  3.30), and H<sub>2</sub>O ( $\delta$  4.35), where the chemical shift is reported with respect to 1% Me<sub>4</sub>Si in CDCl<sub>3</sub>. Additional water to this system does not significantly affect the chemical shifts of any of the protons except H<sub>2</sub>O. The chemical shifts of the water protons vs. water content are shown in Table II. At low water content, the water proton resonance is upfield compared to that for normal bulk water. Further addition of water to the system causes a

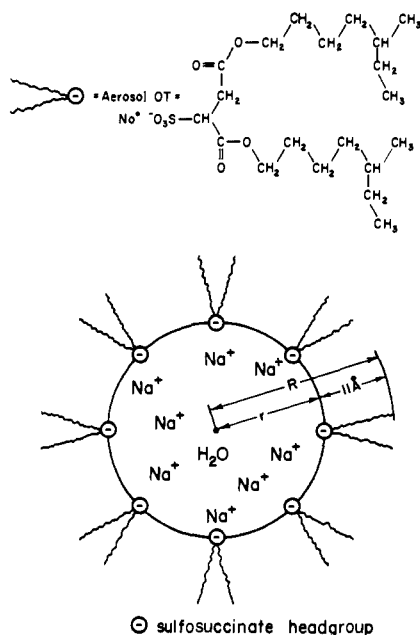


Figure 1. Schematic illustration of an AOT inverted micelle with an aqueous core.

Table I. Micellar Composition<sup>a</sup> and Dimensions for AOT Solutions Employed in the Experiments<sup>b</sup>

	% (v/v) of H <sub>2</sub> O				
	6	2	1	0.5	0.2
N <sub>H<sub>2</sub>O</sub> /N <sub>AOT</sub>	49.3	16.4	8.2	4.1	1.64
N <sub>H<sub>2</sub>O</sub> /micelle	552 570	20 465	2558	319	21
R, Å	84	35.4	23.2	17.1	13.4

<sup>a</sup> AOT content: 3% (w/v). <sup>b</sup> These dimensions are based on data presented in ref 9.

downfield shift of the water peak which approaches that of normal water. Formation of hydrogen bonds usually results in a downfield proton shift<sup>8</sup> (i.e., to larger values). Hence, these NMR results suggest a minimal amount of hydrogen bonding present in the micellar water phase. At low water content (<1%), all of the water molecules are expected to participate in the solvation shell of the counter Na<sup>+</sup> ion or to interact with the polar head group. Similar results have also been observed in the case of very strong electrolyte solutions.<sup>10</sup> Upon complete solvation of the counter ions, additional water is available for hydrogen bonding, resulting in a downfield shift at higher water content. Even in the largest water pools, only one peak is observed for the water protons, resulting in a weight-average resonance detected in the absorption spectrum. The lifetime of the water in both sites is therefore shorter than 10<sup>-4</sup> s.<sup>11</sup>

To further elucidate the role of water in these micellar aggregates, the relaxation rates of water molecules were measured at various water content. The longitudinal nuclear relaxation rate yields information concerning the motion of the molecules in the solution.<sup>10</sup> A change in molecular motion can reflect a change in the structure of the medium,<sup>12</sup> and/or the interactions between the molecules observed and the surrounding environment. The spin-lattice ( $T_1$ ) or the longitudinal relaxation time and the spin-spin ( $T_2$ ) or the transverse

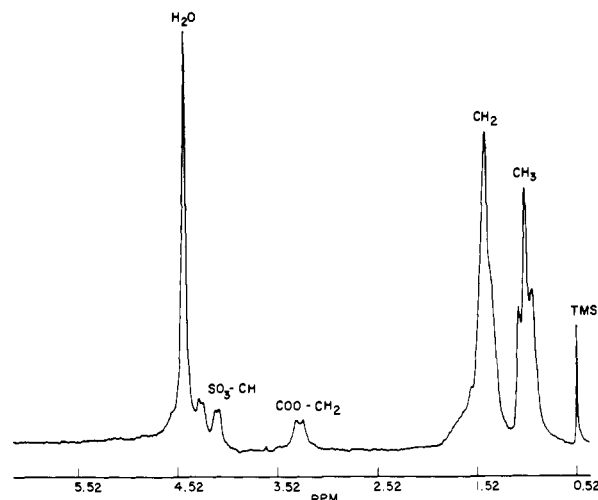


Figure 2. <sup>1</sup>H NMR spectrum of 3% AOT/0.8% H<sub>2</sub>O/C<sub>7</sub>D<sub>16</sub> solutions.

relaxation time of <sup>1</sup>H of the solubilized water in various sizes of water pools are shown in Table III. Increasing the water content in the micellar aggregates increases both  $T_1$  and  $T_2$  relaxation times. The relaxation times are related to molecular motion by the correlation time  $\tau_c$ , which serves as a measure of the average time that two nuclei remain in a given relative orientation. The correlation time depends on the viscosity of the medium and on the size and shape of the molecules involved. For a system of two equal spins ( $I_1 = I_2 = I$ ), where the spins are proton nuclei, the dipole-dipole relaxation mechanism is usually dominant. The intramolecular contribution to relaxation of nucleus I is caused by dissipation of the nuclear spin energy to rotational motion and is given by<sup>13</sup>

$$(1/T_1)_{\text{intra}} = \frac{2\gamma^4\hbar^2 I(I+1)}{5r^6} \times \left( \frac{\tau_c}{1 + \omega^2\tau_c^2} + \frac{4\tau_c}{1 + 4\omega^2\tau_c^2} \right) \quad (1)$$

$$(1/T_2)_{\text{intra}} = \frac{\gamma^4\hbar^2 I(I+1)}{5r^6} \times \left( 3\tau_c + \frac{5\tau_c}{1 + \omega^2\tau_c^2} + \frac{4\tau_c}{1 + 4\omega^2\tau_c^2} \right) \quad (2)$$

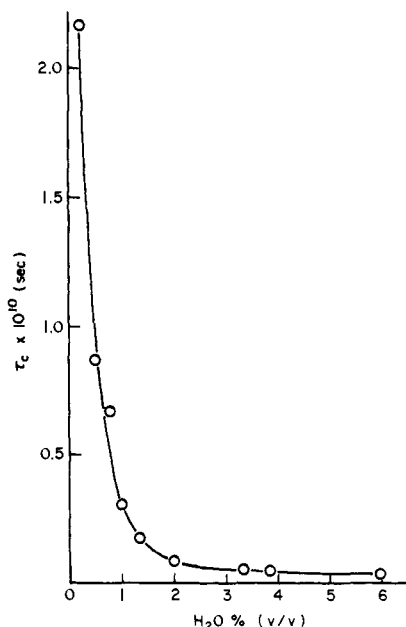
The rotational correlation time  $\tau_c$  for a water molecule in the water pools can be calculated by substituting the experimental  $T_1$  value, the gyromagnetic ratio,  $\gamma$ , and the intramolecular proton-proton distance  $r$  into eq 1. The value  $\omega$  is the nuclear precession frequency. The correlation times for water proton interactions as a function of water content are shown in Figure 3. The change in the rotational correlation time is most significant in a region where the water content of the micelle is relatively small and approaches a plateau at larger radii of the water pools. A break occurs at about 1% H<sub>2</sub>O where the water molecule per sodium ion ratio exceeds 6. Since sodium ion is known to be a water structure forming ion in aqueous solution, the strong ion-dipole interaction will reduce the mobility of water molecules adjacent to the ion and increase the relaxation rates of the <sup>1</sup>H in water.<sup>10,14</sup> At low water content in reversed micelles, the stronger ion-dipole interaction energies compared to dipole-dipole interactions between the water molecules will cause water molecules to participate in the solvation of the counter sodium ions. Water molecules not

Table II. <sup>1</sup>H Chemical Shift of Solubilized Water in the 3% AOT/H<sub>2</sub>O/Heptane Solutions

% H <sub>2</sub> O	0.2	0.5	0.8	1	1.35	2	3.35	3.85	6
$\delta$	4.14	4.25	4.35	4.51	4.52	4.65	4.81	4.87	4.89

**Table III.** Comparison of  $^1\text{H}$  ( $1/T_1$ ) and ( $1/T_2$ ) Relaxation Rates with the Theoretical Values Assuming only a Dipole–Dipole Relaxation Mechanism for the Solubilized  $\text{H}_2\text{O}$  Protons in the Reversed Micelles AOT/ $\text{H}_2\text{O}$ /Heptane

% $\text{H}_2\text{O}$ (v/v)	$(1/T_1)_{\text{obsd}}$	$(1/T_1)_{\text{obsd}} - (1/T_1)_0$	$(1/T_2)_{\text{obsd}}$	$(1/T_2)_{\text{obsd}} - (1/T_2)_0$	$(1/T_2)_{\text{calcd}}$
0.2	12.5	12.1	69.08	68.53	12.1
0.5	5.5	5.1	24.49	23.94	5.1
0.8	4.4	4.0	16.33	15.78	4.0
1	2.2	1.8	15.70	15.15	1.8
1.35	1.45	1.06	12.56	12.01	1.06
2.0	0.9	0.51	12.56	12.01	0.51
3.35	0.7	0.31	8.48	7.93	0.31
3.85	0.65	0.26	6.83	6.67	0.26
6	0.62	0.23	7.22	4.47	0.23

**Figure 3.** The effect of water content on the rotational correlation times  $\tau_c$  in 3% AOT/ $\text{H}_2\text{O}$ / $\text{C}_7\text{D}_{16}$  reversed micelles.

participating in hydration will still undergo binding via ion-dipole forces or via hydrogen bonds to sulfonate or carboxylate groups present in the cavity. The mobility of water molecules engaged in these binding sites is greatly reduced so the correlation time of the  $^1\text{H}$  nuclei of these water molecules is much higher than that of bulk water. Introducing additional water to the system gradually leads to a saturated solvation shell with a concomitant reduction in correlation time. At low water content (i.e., 0.2%) the correlation time for water protons is only a factor of 5 shorter than the rotational time of the overall micelle ( $\tau_r \approx 1 \times 10^{-9}$  s) estimated using the Stokes equation. Hence, at low water content the motion is predominantly influenced by the overall tumbling of the micelle complex. Above 1%  $\text{H}_2\text{O}$ , additional water is free and  $\tau_c$  approaches a value measured for bulk water ( $3 \times 10^{-12}$  s).<sup>15</sup> Similar conclusions have been made regarding water in cells and in protein solutions,<sup>15</sup> namely that a small fraction of water is firmly bound to macromolecules and exhibits extremely short relaxation times (long rotational correlation time). This bound water exchanges rapidly with the bulk water and dominates the observed relaxation processes.

The rotational correlation time  $\tau_c$  obtained from  $T_1$  can be substituted into eq 2 to calculate the spin–spin relaxation time  $T_2$ . Table III shows the calculated and experimental values of  $1/T_2$  in water pools of different sizes. The differences between calculated and experimental values are smaller in larger water pools. The validity of eq 2 in calculating  $T_2$  depends on the

**Table IV.**  $^1\text{H}$  Spin–Lattice Relaxation Times in 3% AOT/ $\text{H}_2\text{O}$ /Heptane Solutions

% $\text{H}_2\text{O}$	$1/T_1, \text{s}^{-1}$				
	$\text{H}_2\text{O}$	$\text{SO}_3\text{CH}$	$\text{COOCH}_2$	$\text{CH}_2$	$\text{CH}_3$
0.5	5.5	7.0	10.2	3.5	1.90
0.8	4.4	8.4	11.3	3.5	1.70
1.0	2.2	7.3	10.6	3.4	1.75
1.35	1.45	7.3	10.5	3.0	1.65
2.0	0.9	5.5	7.0	3.0	1.60
3.35	0.7	5.7	6.1	2.45	1.85
3.85	0.65	5.5	4.8	2.4	1.75
6.0	0.62	3.7	4.5	3.91	1.75

condition that intramolecular dipole–dipole relaxation dominates the spin–spin relaxation. Hence, the deviation of the experimental  $T_2$  value from that predicted from eq 2 indicates that other relaxation mechanisms which cause a fluctuating magnetic field about the perturbed  $^1\text{H}$  nucleus also contribute to the spin–spin relaxation process. The most probable mechanism is relaxation via anisotropic electronic shielding, as the magnetic field experienced by a nucleus depends on its electronic shielding (chemical shifts). An anisotropy in the shielding causes the nuclei to experience a changing magnetic field as the molecule tumbles in solution.<sup>13</sup> In the case of small micelles, where the hydration shell about the sodium ion is incomplete, the shielding is not equal in all directions about the water proton nuclei. This leads to an additional relaxation mechanism in addition to dipole–dipole relaxation. Furthermore, the rapid spin exchange between various environments causes an additional contribution to the transverse relaxation rate. The theoretical approach to this problem has been carried out by Gutowsky,<sup>16</sup> McConnell,<sup>17</sup> and Swift.<sup>18</sup> Finally, the experimental  $T_2$  value is evaluated from the width of the line at half maximum intensity. Inhomogeneity in the magnetic field also causes additional line broadening, resulting in an increase in the apparent relaxation rate.

The spin–lattice relaxation rates ( $1/T_1$ ) of the proton nuclei of the AOT molecules in the reversed micelles are shown in Table IV. Increasing the water content in the micellar aggregates affects only the relaxation rates of those protons adjacent to the polar head groups, while those of the terminal methyl and methylene groups remain unchanged. Since the water molecules are only in contact with the polar head groups, further addition of water to the system increases the fluidity in the center aqueous pool and the interface region. Therefore, the relaxation rates of the protons of water and of the protons adjacent to the polar head groups decrease. The addition of water to the phosphatidyl choline reversed micelles in either diethyl ether,<sup>19</sup> benzene,<sup>20</sup> or carbon tetrachloride<sup>21</sup> is also found to increase the molecular motion of the lipid–water interface. The activity of enzymes bound to the lecithin reversed

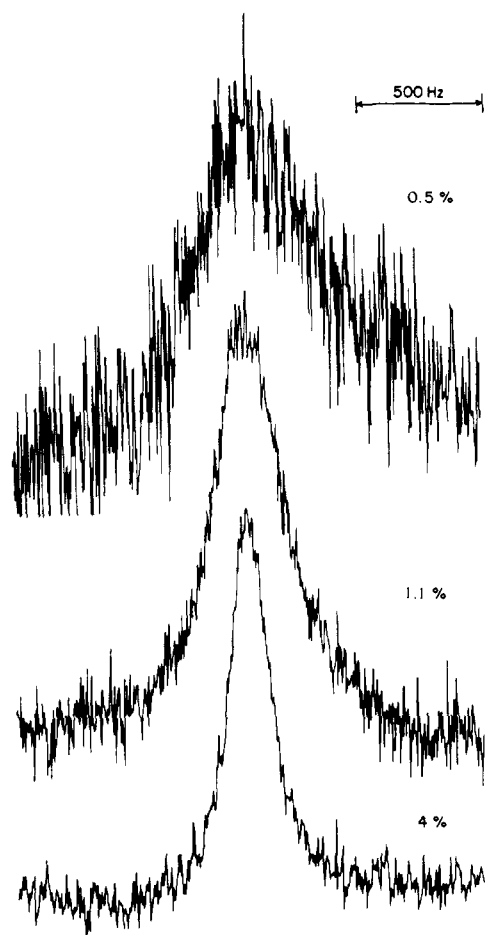


Figure 4. The  $^{23}\text{Na}$  NMR spectra of 3% AOT/ $\text{H}_2\text{O}/\text{C}_7\text{H}_{16}$  solutions.

micelles depends dramatically on the nature of the lipid-water interface.<sup>22,23</sup>

**The Effect of Water on the  $^{23}\text{Na}$  NMR Spectrum.** Since the state and nature of water in reversed micelles are affected significantly by the counter ion, direct studies of the counter ion,  $\text{Na}^+$ , were studied in reversed micelles. Considerable interest<sup>24-26</sup> has focused on the application of nuclear magnetic quadrupole relaxation processes to investigate events occurring at the amphiphile-water interface in these micelles. The  $^{23}\text{Na}$  NMR spectrum of the reversed micelle formed by AOT/ $\text{H}_2\text{O}$ /heptane is shown in Figure 4. A single broad absorption peak is observed in these experiments, and the resonance line width decreases dramatically as the water content of the system increases. Figure 5 shows the dependence of the line width on the water content in reversed micelles. Since the nuclear magnetic relaxation is the result of time-dependent interactions between the nucleus and its surroundings, the rate of relaxation depends on the strength of interaction as well as on the rate of molecular motion. In the case of nuclei possessing electric quadrupole moments, the interaction between the electric quadrupole moment and the electric field gradients at the nuclei usually dominates the relaxation mechanism. Under conditions of extreme narrowing, the relaxation rates may be written<sup>27</sup>

$$1/T_1 = 1/T_2 = \frac{3}{40} (e^2qQ/\hbar)^2 (2I + 3)/I^2 (2I - 1) \tau_c \quad (3)$$

Here,  $I$  is the spin quantum number which is  $\frac{3}{2}$  for  $^{23}\text{Na}$ ,  $eQ$  is the largest component of the electric field gradient tensor being modulated by the molecular motion,  $eQ$  is the electric quadrupole moment, and  $\tau_c$  is the correlation time characterizing the rate of change of the field gradients. In normal micelles in aqueous solutions, it has been found that the rota-

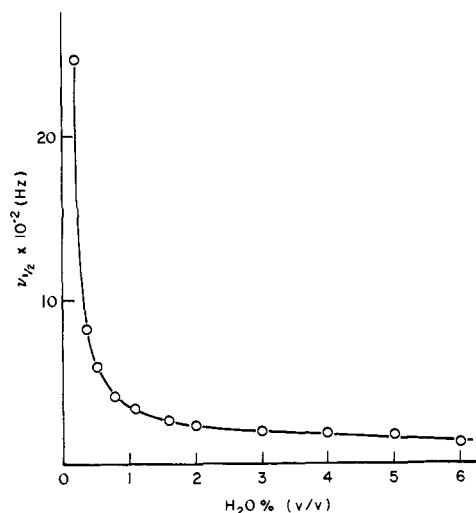


Figure 5. The effect of water on the line width of  $^{23}\text{Na}$  NMR absorption lines.

tional, vibrational, and translational motions of water molecules in the immediate neighborhood of the counter ions affect the fluctuating field gradients and dominate the relaxation<sup>14,28</sup> of the counter ion. In the case of reversed micelles under current study, the marked dependence of the  $^{23}\text{Na}$  NMR line width on the initial water content may occur first from the immobilization of the water molecules around the sodium ion by participating in the hydration shell, a point which has been described previously in the  $^1\text{H}$  NMR data. Secondly, before completion of the solvation shell, electric field gradients arise from the asymmetrical charge and dipole distribution around the sodium nuclei due to the distorted hydration sphere. Finally, successive binding of water molecules to the  $\text{Na}^+$  ion associated at the head group weakens or interrupts the ion-ion coupling within the complex.

On completion of the hydration shell around the counter ion, the  $^{23}\text{Na}$  line width still continues to decrease slowly with increasing amounts of water. At higher water content, a greater percentage of sodium ions could be present as free hydrated ions and exchange rapidly with the bound sodium ion (hydrated ion associates). The relaxation is dominated by the latter class of ions. The line width in the largest water pool is still ten times broader than those in saturated  $\text{NaCl}$  aqueous solutions, which indicates that the mobility of the hydrated sodium ions in water pools with radius  $73 \text{ \AA}$  is still greatly reduced. A similar dependence of the line width on the water content is also found in reversed micelles formed by sodium caprylate/caprylic acid/ $\text{H}_2\text{O}$ .<sup>26</sup>

In the previous discussion, the exchange rate of the sodium between the bound and the free sites is assumed to be rapid and therefore does not contribute to the relaxation mechanism. Hertz<sup>29</sup> has suggested that the exchange process may be distinguished by the temperature dependence of the line width. In the case of rapid exchange, the line width should decrease with increasing temperature, since the correlation time will decrease. On the other hand, for slow exchange, the line width would increase with increasing temperature, since the rate of chemical exchange increases. The dependence of  $^{23}\text{Na}$  line width on temperature at several sizes of water pools in the reversed micelles is shown in Figure 6. Increasing the temperature decreases the resonance line width, and is consistent with the assumption of fast exchange of  $^{23}\text{Na}$  in these solutions.

From the Arrhenius plots in Figure 6, a constant apparent activation energy is calculated. Table V gives the activation energy for the  $^{23}\text{Na}$  relaxation processes in reversed micelles of several sizes. Since the interaction process involved here is

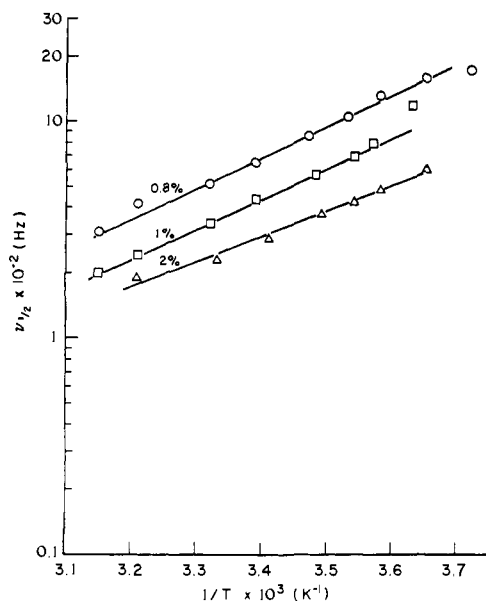


Figure 6. The Arrhenius plot of  $^{23}\text{Na}$  NMR line width vs.  $1/T$  in the AOT/ $\text{H}_2\text{O}/\text{C}_7\text{H}_{16}$  solutions.

Table V. The Apparent Activation Energy for  $^{23}\text{Na}$  Relaxation Process

% $\text{H}_2\text{O}$	0.8	1	2
$E$ , kcal/mol	6.85	6.44	5.42

more complicated than in simple aqueous solution, it can only be concluded that the high activation energies indicate a strong interaction of  $\text{Na}^+$  with the ligands in its environment.<sup>26</sup> Higher activation energies in the smaller size micelles indicate strong binding of the sodium ions, which agrees with the interpretation of the line width data. The activation energies in the large micelles are again higher than those of bulk water (2.5 kcal/mol).

In conclusion,  $^1\text{H}$  and  $^{23}\text{Na}$  NMR relaxation studies indicate that the water in the first hydration shell is highly immobilized due to strong ion-dipole interaction between the counter ion and the water. The rigidity is greatly reduced in both the lipid-water interface and the center water pool when more water is included into the system. However, mobility in the largest water pool is still slower than in bulk water.

**The Extent of Association of  $^{23}\text{Na}^+$  Ion to the Micellar Surface.** Since sodium ions exist both in the free and bound state in reversed micelles, it is important to determine the relative distribution of both states, i.e., the extent of association of  $\text{Na}^+$  to the micellar surface. NMR spectroscopy has been applied successfully to the study of the degree of counter ion binding in the conventional normal micelles; however, difficulties arise when the similar technique was carried out in reversed micellar systems.<sup>30,31</sup>

In this work, the degree of association of the counter ions to the micellar surface is estimated by taking advantage of the difference in relaxation rates of the sodium ions in the two states. Since the exchange between the two sites of sodium ions is a fast process as indicated from the temperature studies, and if we assume only two sites of the sodium ions, the observed line width of  $^{23}\text{Na}$  is then given by<sup>23</sup>

$$\nu_{1/2} = P_b\nu_b + P_f\nu_f \quad (4)$$

where  $P_b$  and  $P_f$  are the mole fractions for the sodium ion in the bound and free states, respectively, and  $\nu_b$  and  $\nu_f$  are the line widths of the sodium ion in the corresponding states. If we assume that the ratio  $\nu_b/\nu_f$  in the reversed micelles is not sig-

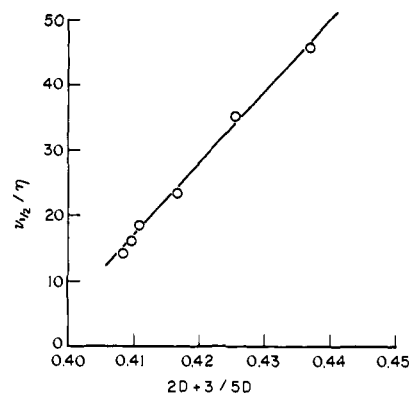


Figure 7. The effect of polarization on  $^{23}\text{Na}$  NMR line width in 0.067 M  $\text{NaCl}/\text{H}_2\text{O}/\text{dioxane}$  solutions.

nificantly different from that in the normal micelles, a reasonable assumption in the case of the largest water pools, then a ratio of approximately 3.1 is obtained from Lindman's work<sup>23</sup> in sodium octyl sulfate and sodium octanoate micelles. The environment of the unbound, hydrated sodium ions in the water pools may significantly differ from that of the ordinary bulk water. The characteristic fluorescent properties of ANS which have been investigated earlier measure the dielectric constant of the water molecules in the largest water pool in the reversed micelles to be 77.9 on Kosower's polarity scale  $Z$  ( $D \sim 17.5$ ). From relaxation studies of electrolytes in nonaqueous solution, a close connection between the quadrupole coupling  $\nu_{1/2}/\eta$  and the polarization produced by the surrounding solvent related to solvent's dielectric constant  $(2D + 3)/5D$  is found.<sup>32,33</sup> This is true provided the quadrupole coupling at the nuclei still arises from ion-solvent interactions instead of ion pair interactions. A plot of  $\nu_{1/2}/\eta$  vs.  $(2D + 3)/5D$  for 0.067 m  $\text{NaCl}$  or  $\text{NaBr}$  (the concentration of  $\text{Na}^+$  in the largest water pool) in  $\text{H}_2\text{O}/\text{dioxane}$  mixture is shown in Figure 7. If we interpolate the dielectric constants of the largest water pool into Figure 7 using the microviscosity data obtained from fluorescence depolarization, then the line width of the free hydrated sodium in the water pools is 44 Hz. The line width of the bound sodium ion is then equal to  $3.1 \times 44$  or 136 Hz. The degree of binding of the counter ions to the micellar surface in the largest water pool could be thus calculated from eq 4, and is found to be 72%.

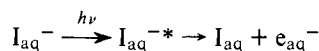
The extent of dissociation of counter ions from the micellar surface calculated in the largest water pool is not significantly different from that of normal micelles. However, since some approximation is involved in the calculation, this should be regarded as an approximation. Furthermore, since the dielectric constant in the water pool is not as large as that in the normal bulk water, the ratio of  $\nu_b/\nu_f$  may actually be smaller, in the case of reversed micelles, since the solvation energy of the sodium ion would be smaller in the water pool. Thus, 72% of ions binding to the micellar surface could only be a lower limit.

**The Absorption Spectra of  $\text{I}^-$  in the Aqueous Core of Reversed Micelles.** The UV absorption spectra of  $5 \times 10^{-4}$  M  $\text{I}^-$  (bulk concentration) in the reversed micelles AOT/ $\text{H}_2\text{O}/\text{heptane}$  was investigated. The absorption maximum and extinction coefficient in micelles of varying size are shown in Table VI. Although the extinction coefficient increases strongly with increasing water content, it is still about 100 times smaller in the largest water pool (6%  $\text{H}_2\text{O}$ ) than it is in pure water. On the other hand, the concentration of water in the micelles only has a small effect on the absorption energy. The absorption spectra of  $\text{I}^-$  in all reversed micelles show a red shift compared to that in pure water. Franck and Platzman<sup>34,35</sup> first proposed that the UV absorption spectrum of iodide ions involves the formation of spherically symmetric excited states

**Table VI.** The Spectral Shift and Extinction Coefficient of  $5 \times 10^{-4}$  M  $I^-$  in the Reversed Micelles and Water

% H <sub>2</sub> O	0.55	0.8	1	1.5	2	3	4	6	100
$\lambda_{\max}$ , nm	236.6	236.8	237.0	237.4	237.7	237.8	238.0	238.0	226.0
$\epsilon$ , M <sup>-1</sup> cm <sup>-1</sup>	7.4	14.9	19.9	35.2	48.4	79.5	105.2	160.8	12 700

centered on the parent atom. These excited states subsequently dissociate into iodine atoms and electrons which are then solvated by the surrounding solvent according to



Stein and Treinin<sup>36-38</sup> later modified the model of Franck and Platzman with the concept of an electron in a box with various radii, a concept first developed by Smith and Symons,<sup>39-41</sup> to successfully interpret features of the spectroscopic data such as the absorption maxima, the effect of temperature, solvent, and added solutes. According to their theory, a major portion of the effect of added solutes is due to the influence of the solute on the structure of the water solvent, thus the solvation environment of the iodide ion is modified, causing a spectroscopic change. The spectral red shift of the iodide ion in the reversed AOT micelles may then occur because of the large number of water molecules associated with the counterions or head groups. The hydrogen-oxygen interaction bonding is decreased and the number of available unbound polar hydrogens increases. Hence a larger proton cavity is formed around the iodide ion and the resulting spectra are slightly shifted to the red. A similar effect has been observed<sup>38</sup> in aqueous iodide solutions due to the presence of the counter cations. The very low spectral transition probability of the iodide ion in reversed micelles could be best explained by the availability of the water molecules to solvate the ground state as well as the excited state of the iodide ion. Lack of water molecules about the iodide ion distorts the wave function of the ground and excited states so that the transition becomes highly improbable at low water content. Addition of water to the system increases the polarity of the water pools, so that the transition probability is higher at larger water content. A similar conclusion regarding the nature of water in reversed micelles formed by phosphatidyl choline in diethyl ether is also attained by Wells<sup>19</sup> on probing the interior water pool by CoCl<sub>2</sub>. Water when first added to reversed micelles tends to be present as a tightly bound water shell around the polar head group. Few water molecules are available to solvate CoCl<sub>2</sub>, and therefore a tetrahedral blue complex of Co<sup>2+</sup> is formed which absorbs strongly at 650 nm. Upon completion of the first hydration shell of the micelle, water molecules start to complex with Co<sup>2+</sup>, forming a pink octahedral complex CoCl<sub>2</sub>·6H<sub>2</sub>O, with a concomitant decrease in the molar absorptivity in the red.

#### IV. Conclusion

Spectroscopic studies of the water phase in reversed micelles demonstrate that the water aggregate in these systems is radically different from that of bulk water. <sup>1</sup>H NMR studies measuring chemical shifts of reversed micellar systems indicate environmental changes only in H<sub>2</sub>O and <sup>1</sup>H head group of amphiphile. The effect of increasing H<sub>2</sub>O content in the micellar interior on <sup>1</sup>H nuclear longitudinal and transverse relaxation rates demonstrates that the nature of H<sub>2</sub>O is highly immobilized and mobility increases with increasing water content. From our measured values,  $\tau_{\text{rotation}}$  decreases from  $2 \times 10^{-10}$  s to approximately  $3.9 \times 10^{-12}$  s, a value obtained for bulk water. The value for  $\tau_{\text{rot}}$  dramatically increases as the H<sub>2</sub>O to Na<sup>+</sup> ratio increases up to a value of approximately 6 (the hydration number of Na<sup>+</sup>) after which  $\tau_{\text{rot}}$  asymptotically approaches the value for bulk H<sub>2</sub>O.

From the deviation of the  $1/T_2$  results from a simple dipole-dipole relaxation mechanism, a substantial contribution of an anisotropic electronic shielding of the H<sub>2</sub>O is indicated.

From <sup>23</sup>Na relaxation measurements, an analogous decrease in the  $1/T_2$  is observed with increasing H<sub>2</sub>O content. This data is consistent with a rapid change in solvent mobility upon saturation of the hydration sphere of the Na<sup>+</sup> ion.

Measurement of the I<sup>-</sup> electronic absorption spectrum indicates that a minimal hydrogen-bonded aqueous matrix is present at low water content (less than 6H<sub>2</sub>O/Na<sup>+</sup>) and upon increasing the H<sub>2</sub>O/Na<sup>+</sup> ratio the I<sup>-</sup> spectrum appears to be more like that of an aqueous I<sup>-</sup> spectrum. This data is consistent with the chemical shifts of <sup>1</sup>H of H<sub>2</sub>O in this system, which move downfield upon increasing water content, consistent with a greater amount of hydrogen bonding found in the aqueous matrix.

Spectroscopic studies indicate that the properties of bulk water do not appear in reversed micelle systems until the H<sub>2</sub>O/Na<sup>+</sup> ratio in the micellar core exceeds 6.

**Acknowledgment.** The research described herein was supported by the Division of Physical Research of the U.S. Energy Research and Development Administration. This is Radiation Laboratory Document No. NDRL-1732.

#### References and Notes

- P. A. Winsor, *Chem. Rev.*, **68**, 1 (1968).
- C. Singletary, *J. Am. Oil Chem. Soc.*, **32**, 446 (1955).
- P. H. Elworthy, A. T. Florence, and C. B. MacFarlane, "Solubilization of Surface Active Agents", Chapman and Hall, London, 1968.
- (a) J. H. Fendler, *Acc. Chem. Res.*, **9**, 153 (1976); (b) J. H. Fendler and E. J. Fendler, "Catalysis in Micellar and Macromolecular Systems", Academic Press, New York, N.Y., 1975.
- B. Chance, *Proc. Natl. Acad. Sci. U.S.A.*, **67**, 560 (1970).
- M. Wong, M. Gratzel, and J. K. Thomas, *J. Am. Chem. Soc.*, **98**, 2391 (1976); M. Wong and J. K. Thomas, Proceedings of Micelle Symposium, Albany, N.Y., 1976.
- H. Christen, H.-F. Eicke, H. Hammerichand, and U. Strahm, *Heiv. Chim. Acta*, **59**, 1297 (1976).
- E. D. Becker, "High Resolution NMR", Academic Press, New York, N.Y., 1972.
- P. Elwall, L. Mandell, and K. Fontell, *J. Colloid Interface Sci.*, **33**, 215 (1970); M. B. Mathews and E. J. Hirschhorn, *ibid.*, **8**, 86 (1953).
- H. G. Hertz, "Progress in NMR Spectroscopy", Vol. III, Pergamon Press, Oxford, 1967.
- D. Eisenberg and W. Kaufman, "The Structure and Properties of Water", Oxford, 1969.
- H. G. Hertz, *Ber. Bunsenges. Phys. Chem.*, **68**, 907 (1964).
- T. James, "NMR in Biochemistry", Academic Press, New York, N.Y., 1975.
- C. Deverell, "Progress in NMR Spectroscopy", Vol. IV, Pergamon Press, Oxford, 1967.
- R. Cooke and I. P. Kuntz, *Annu. Rev. Biophys. Bioeng.*, **4**, 267 (1975).
- H. S. Gutowsky, O. W. McCall, and C. P. Slichter, *J. Chem. Phys.*, **21**, 279 (1953).
- H. M. McConnell, *J. Chem. Phys.*, **28**, 430 (1958).
- T. J. Swift and R. E. Connick, *J. Chem. Phys.*, **41**, 2553 (1964).
- M. A. Wells, *Biochemistry*, **13**, 2943 (1974).
- W. V. Walter and R. G. Hayes, *Biochim. Biophys. Acta*, **249**, 528 (1971).
- B. M. Fung and J. L. McAdams, *Biochim. Biophys. Acta*, **451**, 313 (1976).
- R. L. Mlsiorowski and M. A. Wells, *Biochemistry*, **12**, 967 (1973).
- P. H. Poon and M. A. Wells, *Biochemistry*, **13**, 4928 (1974).
- H. Gustavsson and B. Lindman, *J. Am. Chem. Soc.*, **97**, 3923 (1975).
- B. Lindman and P. Ekwall, *Mol. Cryst.*, **5**, 79 (1968).
- B. Lindman and P. Ekwall, *Kolloid Z. Z. Polym.*, **234**, 1115 (1969).
- A. Abragam, "The Principles of Nuclear Magnetism", Clarendon Press, Oxford, 1961.
- G. Lindblom and B. Lindman, *Berichte vom VI. Internationalen Kongre B für Grenzflächenaktive Stoffe, Zurich, vom II. bis 15. September, 1972.*
- H. G. Hertz, *Ber. Bunsenges. Phys. Chem.*, **67**, 311 (1963).
- G. Lindblom, B. Lindman, and L. Mandell, *J. Colloid Interface Sci.*, **34**, 262 (1970).

- (31) G. Lindblom and B. Lindman, *J. Phys. Chem.*, **77**, 2531 (1973).  
 (32) M. H. Cohen and F. Relf, *Solid State Phys.*, **5**, 321 (1957).  
 (33) R. E. Richards and B. A. Yorke, *Mol. Phys.*, **10**, 551 (1966).  
 (34) J. Franck and R. L. Platzman, "Theory of the Absorption Spectra of Halide Ions in Solutions", Farkas Memorial Vol., Jerusalem, 1952.  
 (35) J. Franck and R. L. Platzman, *Z. Phys.*, **138**, 411 (1954).  
 (36) J. Jortner, B. Raz, and G. Stein, *Trans. Faraday Soc.*, **56**, 1273 (1960).  
 (37) J. Jortner, B. Raz, and G. Stein, *J. Chem. Phys.*, **34**, 1455 (1961).  
 (38) G. Stein and A. Treinin, *Trans. Faraday Soc.*, **56**, 1393 (1960).  
 (39) M. Smilth and M. C. R. Symons, *Discuss. Faraday Soc.*, **24**, 206 (1967).  
 (40) M. Smith and M. C. R. Symons, *Trans. Faraday Soc.*, **54**, 338 (1958).  
 (41) M. Smith and M. C. R. Symons, *J. Chem. Phys.*, **25**, 1074 (1956).

## Introduction, Modification, and Characterization of Functional Groups on the Surface of Low-Density Polyethylene Film

James R. Rasmussen,<sup>1</sup> Erwin R. Stedronsky, and George M. Whitesides\*

*Contribution from the Department of Chemistry, Massachusetts Institute of Technology, Cambridge, Massachusetts 02139. Received October 18, 1976*

**Abstract:** Initial oxidation of low-density polyethylene film with concentrated chromic acid solution at temperatures between 25 and 75 °C, followed by further oxidation with 70% aqueous nitric acid at 50 °C, generates a surface containing a relatively small number of different types of functional groups. The identities and relative numbers of these functional groups have been established using ATR IR spectroscopy and chemical derivatization. The surface functionality consists primarily of carbonyl derivatives, with approximately 60% of these present as carboxylic acid groups and 40% as ketones or aldehydes. Alcohols do not seem to be present. The absolute number of carboxylic acid groups generated at the surface was assayed using two independent fluorimetric techniques to be approximately  $2 \times 10^{15}/\text{cm}^2$  of geometrical film area: since the surface is rough, the actual surface density of carboxyl groups is lower than this number. Several procedures have been developed which use these carboxylic acid groups as the basis for further chemical modification of the polymer surface.

The surface composition and structure of solid organic polymers influence many of their properties and uses. Wetting,<sup>2</sup> weathering,<sup>3</sup> permeation,<sup>4</sup> adhesion,<sup>5,6</sup> friction,<sup>6</sup> electrostatic charging,<sup>7</sup> and dye adsorption<sup>5</sup> are examples of processes important in engineering applications of polymers whose characteristics are determined, in part, by surface constitution. Surface functionality influences biocompatibility,<sup>8</sup> especially thromboresistance<sup>9</sup> and cellular attachment.<sup>10</sup> Solid-phase organic synthesis requires high-yield reactions to introduce and modify polymer functionality, and methods to control the interactions between pendant functional sites.<sup>11</sup>

Polymeric materials having particular surface properties are presently developed empirically. It is difficult to construct and test hypotheses relating the molecular structure of a polymer surface to its macroscopic surface properties because it has not been possible to obtain polymers with surfaces having well-defined functionality. The purpose of the work described in this and the accompanying paper<sup>12</sup> is the development of techniques for generating, modifying, and characterizing functionality at the surface of low-density polyethylene film.

The problems encountered in manipulating surface functionality on organic polymers differ in three respects from those familiar in organic solution chemistry. First, to be useful, reactions employed to create or modify groups at a surface must proceed in high yields, because it is impossible to separate and purify the products of these reactions. Second, characterization of surface functionality is difficult, both because the absolute number of surface groups is low and because the bulk polymer must be distinguished from the surface. Third, the three-dimensional spatial distribution of functional groups in the surface region—a problem having no counterpart in solution chemistry—is an important consideration in surface chemistry. In fact, the definition of the word "surface" for an organic polymer is not straightforward. In this paper, we use the words "surface" and "interface" interchangeably, and define both operationally in terms of a particular type of experiment which

forms the basis for many of the reactions used: consider a hydrophobic organic polymer (polyethylene) in contact with a polar, nonswelling solvent (water). We define the "surface" of the polymer to be that part which is accessible to reagents that are soluble in water, but insoluble in polyethylene. This definition of a polymer surface has shortcomings: it is not applicable to a polymer which is swelled by the solution. It is ambiguous if thermal motion of the polymer chains at the surface transports functional groups from the bulk to the surface and vice versa with a rate comparable to a process used to test for interaction between a surface functional group and a reagent present in solution. Many water-soluble reagents have low but finite solubility in hydrocarbons, and presumably in polyethylene, and it is difficult to establish that a reagent is completely insoluble in the polymer. Nonetheless, this definition suggests experimental approaches to the generation and modification of surface functionality. It also emphasizes the importance of the three-dimensional distribution of functional groups at the polymer-solvent interface. In principle, functional groups at a well-defined polymer surface might be restricted to a coherent monolayer (Figure 1A); alternatively, at a poorly defined surface, the functional groups might be distributed between the polymer-water interface, the bulk polymer, and (by tethering polymer chains) the solvent (Figure 1B). Although these two distributions might not behave differently in many practical applications, the simpler, more ordered one is preferable in studies designed to test the influence of molecular surface structure on macroscopic properties.

We have chosen to investigate the surface chemistry of polyethylene rather than some other polymer for several reasons. It is readily available, inexpensive, and relatively well-characterized.<sup>13-15</sup> It is sufficiently strong mechanically that it can be handled without special precautions, but it is at the same time conveniently flexible. Polyethylene has few functional groups other than carbon-carbon and carbon-hydrogen single bonds, and its chemistry would be expected to resemble the extensively studied solution chemistry of hydrocarbons.